STUDY OF ORBITAL ELEMENTS ON THE NEIGHBOURHOOD OF A FROZEN ORBIT

Paula Cristiane Pinto Mesquita Pardal

Instituto Nacional de Pesquisas Espaciais – DMC-INPE – Brazil
paula@dem.inpe.br

Hélio Koiti Kuga

Instituto Nacional de Pesquisas Espaciais – DMC-INPE – Brazil
hkk@dem.inpe.br

Rodolpho Vilhena de Moraes

Grupo de Dinâmica Orbital e Planetologia, DMA-FEG-UNESP
rodolpho@feg.unesp.br

Abstract: *Frozen orbits are studied, including perturbations due to J5 harmonic and atmospheric drag. Non-singular variables are introduced according to non-singular theory used at INPE Satellite Tracking and Control Center (CRC). Using CBERS-1 (China Brazil Earth Resources Satellite) satellite's data, results are compared with those used nowadays at the INPE CRC. The keplerian elements studied are the eccentricity, the argument of perigee and the semi-major axis. Terms up to the J5 order for the geopotential model are considered. The atmospheric drag model used is a classical one and provides a good indicative for the order of the drag perturbations on the orbital elements.*

1 Introduction

If perturbations are not taken into account, the orbital motion of artificial satellites would be ellipses with constant sizes and eccentricities in permanent planes, and the satellites would stay on these orbits indefinitely. The principal effects that make the orbit changes are the non homogeneity of the Earth's mass distribution, the solar-moon attraction, the solar radiation pressure (direct and albedo effects and shadowing), the atmospheric drag, forces due to the Earth's tides, Poynting Robertson drag, Yarkovsky effect and others. For orbital control purposes, it can be important that some elements stay "frozen" in order to make easier some adjustment maneuvers. Specially, for maneuvers that have being carried out by INPE with the satellite CBERS-1, it is important that the perigee stays "frozen", that is, with a constant value.

For several applications, on the contrary of natural bodies cases, which distances between themselves are very large in comparison with their sizes, the artificial satellites are so close that geopotencial secondary terms cannot be neglected. The observations of the motion of some natural bodies were so imprecise that an approximated theory was enough to describe the diversion noticed. However, the precision on artificial satellites observations is very high and, by this reason, the study of the motion of the satellites assuming an almost spherical body potential field has developed since the first satellite launch.

The principal aims here are three. The first is to include perturbations due to J5 harmonic and atmospheric drag in the equations of frozen orbits. The second is to introduce non-singular variables and equations, which describe the behavior of the orbital elements of an artificial satellite in the neighbourhood of a frozen orbit. And the third is to compare the obtained solutions with the ones used nowadays at INPE Satellite Tracking and Control Center (CRC), for CBERS-1 satellite.

Brouwer solution (Brouwer, 1959) presents clear analytic expressions, as functions of time, to the variation of the classic orbital elements (a, e, i, ω, Ω, τ) due to the non-uniform Earth's mass distribution. These analytical formulas allow carrying out the analysis of the temporal behavior of these keplerian elements, as well as the magnitude of the perturbations due to the geopotential. In this paper, the terms of long period perturbations for eccentricity and for argument of perigee up to J5 were developed analytically, through Brouwer´s theory.

Brouwer and Hori solution (Brouwer and Hori, 1961) presents a model that assumes that the atmospheric density decreases exponentially while the height of the satellite increases. It also connects the effects of the perturbations due to Earth's oblateness with the effects of the perturbations due to the atmospheric drag in one unique solution. Coupling terms are considered in the solution yet, and perturbations due to the atmospheric drag were included in the equations of the Brouwer´s theory due to the geopotential considering explicitly terms up to J5. This paper takes into account drag effects only for long period terms.

Using FORTRAN language, these equations have been coded. The program has been tested for several situations and a test for validation was performed. Aiming orbital maneuvers to be conducted by the INPE CRC, and after several tests, the model was made "functionally" valid for the CBERS-1 satellite.

Nevertheless, INPE´s Satellite Tracking and Control Center uses the non-singular theory on space missions which apply the frozen orbits theory concepts, considering only perturbations due to the geopotential up to J3. Brouwer and Brouwer and Hori theories are the same theories used at INPE CRC, but written on a different way and using another set of variables (Raimundo, 2004). Here, the equations given in their theories are expressed in terms of non-singular variables and the solution is obtained, including perturbation due to atmospheric drag and terms due to geopotential up to J5 order.

2 Frozen orbits

A frozen orbit is characterized by keeping (or trying keeping) constant the argument of perigee and eccentricity of the orbit. In this way, for a given latitude, the satellite always passes at the same altitude, benefiting the users by this regularity. That is, this type of orbit maintains the satellite altitude almost constant over any point on Earth's surface. The design of frozen orbits involves selecting the correct values of eccentricity and argument of perigee, for a given semi major axis and orbital inclination. Up to J3 terms, the following system of nonlinear perturbation equations are satisfied (Cutting et. al., 1978)

$$\frac{d\omega}{dt} = \frac{3nJ_2R_T^2}{a^2(1-e^2)^2}\left(1-\frac{5}{4}sin^2 i\right)\left\{1+\frac{J_3R_T}{2J_2a(1-e^2)}\left(\frac{sin^2 i - e^2\cos^2 i}{esini}\right)sin\omega\right\}$$

$$\frac{de}{dt} = \frac{3nJ_3R_T^3 sini}{2a^3(1-e^2)^2}\left(1-\frac{5}{4}sin^2 i\right)\cos\omega \tag{1}$$

where:

a: semi major axis
e: eccentricity
i: orbital inclination
ω: argument of perigee
R_T: Earth´s equatorial radius
$n = \sqrt{\frac{\mu}{a^3}}$: mean motion
μ: Earth´s gravitational constant
J_2: second gravity coefficient
J_3: third gravity coefficient

For argument of perigee values equal to 90º and 270º, the eccentricity perturbations vanish.

3 Brouwer solution – Long period terms due to J3 and J5

Following the development that Brouwer suggested, the next expressions are obtained from the equations that provide secular and long period terms for perturbations due to the geopotential only. For the eccentricity and the argument of perigee variations we have:

$$\dot{\omega} = \frac{3nJ_2R_T^2}{a^2(1-e^2)^2}\left(1-\frac{5}{4}sin^2 i\right)\left\{\begin{array}{l} 1+\dfrac{J_3R_T}{2J_2a(1-e^2)}\left(\dfrac{sin^2 i - e^2\cos^2 i}{esini}\right)sin\omega + \\ \dfrac{J_5R_T^3}{J_2a^3(1-e^2)^3}\left\{\begin{array}{l} \dfrac{5}{64}\left[\begin{array}{l}\left(\dfrac{(1-e^2)sini}{e}-\dfrac{e\cos^2 i}{sini}\right)\times \\ (4+3e^2)+esini(26+9e^2)\end{array}\right]\times \\ \left(1-9\cos^2 i-\dfrac{24\cos^4 i}{1-5\cos^2 i}\right)- \\ \dfrac{15}{32}e\cos^2 isini(4+3e^2)\times \\ \left(3+\dfrac{16\cos^2 i}{1-5\cos^2 i}+\dfrac{40\cos^4 i}{(1-5\cos^2 i)^2}\right)\end{array}\right\}sin\omega \end{array}\right\}$$

$$\dot{e} = \frac{3nJ_2R_T^2}{a^2(1-e^2)^2}\left(1-\frac{5}{4}sin^2 i\right)\left[\begin{array}{l}\dfrac{J_3R_T}{2J_2a}sini+\dfrac{5}{32}\dfrac{J_5R_T^3}{J_2a^3(1-e^2)^3}\times \\ sini(4+3e^2)\left(\dfrac{1-9\cos^2 i-24\cos^4 i}{1-5\cos^2 i}\right)\end{array}\right]\cos\omega \tag{2}$$

where

J_5: fifth gravity coefficient.

4 Brouwer and Hori solution

Let´s introduce, again explicitily, the expressions connected to the atmospheric drag disturbing effects on the equations for the eccentricity, the argument of perigee and the semi-major axis. Their effects will be taken into account only for long period terms, because these terms were considered when the perturbations due to the geopotential up to J5 were included. Because of this, the perturbations considered in the semi-major axis were just due to the atmospheric drag. That is, the geopotential perturbations does not generated long period terms disturbing such keplerian element.

Following the development that Brouwer and Hori suggested, the next expressions are obtained from the equations that provide long period terms for perturbations due to the geopotential and atmospheric drag. For the eccentricity, the argument of perigee and the semi-major axis variations we have

$$
\begin{aligned}
\dot{\omega} = {} & \frac{3nJ_2R_T^2}{a^2(1-e^2)^2}\left(1-\frac{5}{4}sin^2 i\right)\Bigg\{1+\frac{J_3R_T}{2J_2a(1-e^2)}\left(\frac{sin^2 i-e^2\cos^2 i}{esini}\right)sin\omega + \\
& \frac{J_5R_T^3}{J_2a^3(1-e^2)^3}\Bigg\{\frac{5}{64}\Bigg[\left(\frac{(1-e^2)sini}{e}-\frac{e\cos^2 i}{sini}\right)(4+3e^2)+esini(26+9e^2)\Bigg]\times \\
& \left(1-9\cos^2 i-\frac{24\cos^4 i}{1-5\cos^2 i}\right)-\frac{15}{32}e\cos^2 isini(4+3e^2)\left(3+\frac{16\cos^2 i}{1-5\cos^2 i}+\frac{40\cos^4 i}{(1-5\cos^2 i)^2}\right)\Bigg\}sin\omega\Bigg\}+ \\
& A\frac{J_2R_T^2}{2a^2(1-e^2)^2}\left(\frac{\mu}{a}\right)^{1/2}\exp(-\alpha a)\Bigg\{-\frac{1}{e^2}\left(\frac{3}{2}-\frac{3}{2}\cos^2 i\right)\Bigg[\frac{1}{2}+\left(-\frac{1}{24}+\frac{11}{12}\alpha a+\frac{5}{24}\alpha^2a^2\right)e^2+ \\
& \left(-\frac{1583}{768}-\frac{233}{128}\alpha a-\frac{3}{8}\alpha^2a^2+\frac{143}{128}\alpha^3a^3+\frac{13}{2304}\alpha^4a^4\right)e^4\Bigg]+\frac{1}{e^2(1-e^2)}\left(\frac{3}{2}-\frac{3}{2}\cos^2 i\right)\times \\
& \Bigg[\frac{1}{2}+\left(\frac{1}{8}+\frac{3}{4}\alpha a+\frac{1}{8}\alpha^2a^2\right)e^2+\left(-\frac{667}{768}-\frac{95}{192}\alpha a-\frac{241}{384}\alpha^2a^2+\frac{49}{576}\alpha^3a^3+\frac{11}{2304}\alpha^4a^4\right)e^4\Bigg]- \\
& \left(\frac{3}{2}-\frac{3}{2}\cos^2 i\right)\Bigg[\frac{1}{2}+\left(\frac{31}{24}+\frac{19}{12}\alpha a+\frac{1}{24}\alpha^2a^2\right)e^2+ \\
& \left(-\frac{187}{768}+\frac{49}{192}\alpha a+\frac{123}{128}\alpha^2a^2+\frac{97}{576}\alpha^3a^3-\frac{5}{2304}\alpha^4a^4\right)e^4\Bigg]-(3-\cos^2 i)\times \\
& \Bigg[\left(-\frac{5}{8}+\frac{1}{4}\alpha a+\frac{1}{8}\alpha^2a^2\right)e^2+\left(-\frac{3}{32}-\frac{3}{16}\alpha a-\frac{5}{16}\alpha^2a^2+\frac{3}{16}\alpha^3a^3+\frac{1}{96}\alpha^4a^4\right)e^4\Bigg]+ \\
& \Bigg[\frac{1}{8}\left(1-11\cos^2 i-\frac{40\cos^4 i}{1-5\cos^2 i}\right)-\frac{5J_4}{24J_2^2}\left(1-3\cos^2 i-\frac{8\cos^4 i}{1-5\cos^2 i}\right)\Bigg]\times \\
& \Bigg[4+\left(-1+\alpha^2a^2\right)e^2+\left(-\frac{3}{16}-\frac{3}{8}\alpha^2a^2+\frac{1}{16}\alpha^4a^4\right)e^4\Bigg]\times \\
& \Bigg[\frac{1}{8}\left(1-33\cos^2 i-\frac{200\cos^4 i}{1-5\cos^2 i}-\frac{200\cos^6 i}{\left(1-5\cos^2 i\right)^2}\right)-\frac{5J_4}{24J_2^2}\left(1-9\cos^2 i-\frac{40\cos^4 i}{1-5\cos^2 i}-\frac{80\cos^6 i}{\left(1-5\cos^2 i\right)^2}\right)\Bigg]\times \\
& \Bigg[(1-\alpha a)e^2+\left(\frac{1}{8}+\frac{5}{8}\alpha a+\frac{1}{8}\alpha^2a^2-\frac{1}{8}\alpha^3a^3\right)e^4\Bigg]\Bigg\}sin2\omega
\end{aligned}
\tag{3}
$$

$$
\begin{aligned}
\dot{e} = & -\frac{3nJ_2R_T^2}{a^2(1-e^2)^2}\left(1-\frac{5}{4}sin^2 i\right)\left\{\frac{J_3R_T}{2J_2a}sini+\frac{5}{32}\frac{J_5R_T^3}{J_2a^3(1-e^2)^3}\times\right. \\
& \left[(4+3e^2)sini\left(\frac{1-9\cos^2 i-24\cos^4 i}{1-5\cos^2 i}\right)\right]\cos\omega+ \\
& \frac{1-e^2}{e\sqrt{\mu a}}\left(A\mu\exp(-\alpha a)\right)\left\{\left[1+\left(\frac{3}{4}\alpha a-\frac{1}{4}\alpha^2a^2\right)e^2+\left(\frac{21}{64}+\frac{3}{8}\alpha a+\frac{9}{32}\alpha^2a^2+\frac{1}{8}\alpha^3a^3+\frac{1}{64}\alpha^4a^4\right)e^4\right]+\right. \\
& \frac{J_2R_T^2}{2a^2(1-e^2)^2}\left(\frac{3}{2}-\frac{3}{2}\cos^2 i\right)\left(\frac{1}{2}+\frac{7}{8}\alpha a+\frac{1}{4}\alpha^2a^2-\frac{1}{24}\alpha^3a^3\right)e^2+ \\
& \left.\left(\frac{21}{256}-\frac{93}{256}\alpha a+\frac{27}{128}\alpha^2a^2+\frac{39}{128}\alpha^3a^3-\frac{65}{768}\alpha^4a^4-\frac{1}{256}\alpha^5a^5\right)e^4\right]\cos 2\omega+ \\
& \frac{J_2R_T^2}{2a^2(1-e^2)^2}\left\{\left[\frac{1}{8}\left(1-11\cos^2 i-\frac{40\cos^4 i}{1-5\cos^2 i}\right)-\frac{5J_4}{12J_2^2}\left(1-3\cos^2 i-\frac{8\cos^4 i}{1-5\cos^2 i}\right)\right]\times\right. \\
& \left[\left(\frac{3}{2}+2\alpha a+\frac{1}{2}\alpha^2a^2\right)e^2+\left(-\frac{3}{16}-\frac{1}{2}\alpha a+\frac{5}{8}\alpha^2a^2+\frac{1}{2}\alpha^3a^3+\frac{1}{16}\alpha^4a^4\right)e^4\right]\cos 2\omega- \\
& \left.\left.\frac{aJ_3}{J_2^2R_T}sini\left[\left(\frac{3}{2}+2\alpha a+\frac{1}{2}\alpha^2a^2\right)e+\left(-\frac{27}{16}-\frac{5}{2}\alpha a+\frac{1}{8}\alpha^2a^2+\frac{1}{2}\alpha^3a^3-\frac{1}{16}\alpha^4a^4\right)e^3\right]sin\omega\right\}\right\}- \\
& \frac{1}{e}\sqrt{\frac{1-e^2}{\mu a}}\left(-A\mu\exp(-\alpha a)\right)\left\{\sqrt{1-e^2}\left[1+\left(-\frac{1}{4}+\frac{1}{4}\alpha^2a^2\right)e^2+\left(-\frac{3}{64}-\frac{3}{32}\alpha^2a^2+\frac{1}{64}\alpha^4a^4\right)e^4\right]+\right. \\
& \frac{J_2R_T^2}{2a^2(1-e^2)^{3/2}}\left(\frac{3}{2}-\frac{3}{2}\cos^2 i\right)\left(\frac{1}{6}+\frac{17}{24}\alpha a+\frac{5}{12}\alpha^2a^2-\frac{1}{24}\alpha^3a^3\right)e^2+ \\
& \left.\left(-\frac{179}{768}-\frac{7}{768}\alpha a-\frac{133}{384}\alpha^2a^2+\frac{311}{1152}\alpha^3a^3+\frac{95}{2304}\alpha^4a^4-\frac{1}{256}\alpha^5a^5\right)e^4\right]\cos 2\omega+ \\
& \frac{J_2R_T^2}{2a^2(1-e^2)^2}\left\{\left[\frac{1}{8}\left(1-11\cos^2 i-\frac{40\cos^4 i}{1-5\cos^2 i}\right)-\frac{5J_4}{12J_2^2}\left(1-3\cos^2 i-\frac{8\cos^4 i}{1-5\cos^2 i}\right)\right]\times\right. \\
& \left[\left(-\frac{5}{2}+2\alpha a+\frac{1}{2}\alpha^2a^2\right)e^2+\left(\frac{1}{16}-\frac{5}{4}\alpha a-\frac{9}{8}\alpha^2a^2+\frac{1}{4}\alpha^3a^3+\frac{1}{16}\alpha^4a^4\right)e^4\right]\cos 2\omega- \\
& \left.\frac{aJ_3}{J_2^2R_T}sini\left[\left(-\frac{3}{2}+\alpha a+\frac{1}{2}\alpha^2a^2\right)e+\left(\frac{27}{16}-\frac{13}{8}\alpha a-\frac{3}{2}\alpha^2a^2+8\alpha^3a^3+\frac{1}{16}\alpha^4a^4\right)e^3\right]sin\omega\right\}
\end{aligned}
$$

$$
\begin{aligned}
\dot{a} = & -2\sqrt{\mu a}A\exp(-\alpha a)\times\left\{\left[1+\left(\frac{3}{4}+\alpha a+\frac{1}{4}\alpha^2a^2\right)e^2+\right.\right.\\
& \left.+\left(\frac{21}{64}+\frac{3}{8}\alpha a+\frac{9}{32}\alpha^2a^2+\frac{1}{8}\alpha^3a^3+\frac{1}{64}\alpha^4a^4\right)e^4\right]+\\
& +\frac{J_2{R_T}^2}{2a^2(1-e^2)^2}\left(\frac{3}{2}-\frac{3}{2}\cos^2 i\right)\left[\left(\frac{1}{2}+\frac{7}{8}\alpha a+\frac{1}{4}\alpha^2a^2-\frac{1}{24}\alpha^3a^3\right)e^2+\right.\\
& \left.+\left(\frac{21}{256}-\frac{93}{256}\alpha a+\frac{27}{128}\alpha^2a^2+\frac{39}{128}\alpha^3a^3-\frac{65}{768}\alpha^4a^4-\frac{1}{256}\alpha^5a^5\right)e^4\right]\cos 2\omega+\\
& +\frac{J_2{R_T}^2}{2a^2(1-e^2)^2}\left\{\left[\frac{1}{8}\left(1-11\cos^2 i-\frac{40\cos^4 i}{1-5\cos^2 i}\right)-\frac{5}{12}\frac{J_4}{{J_2}^2}\left(1-3\cos^2 i-\frac{8\cos^4 i}{1-5\cos^2 i}\right)\right]\times\right.\\
& \times\left[\left(\frac{3}{2}+2\alpha a+\frac{1}{2}\alpha^2a^2\right)e^2+\left(-\frac{3}{16}-\frac{1}{2}\alpha a+\frac{5}{8}\alpha^2a^2+\frac{1}{2}\alpha^3a^3+\frac{1}{16}\alpha^4a^4\right)e^4\right]\cos 2\omega-\\
& \left.\left.-\frac{aJ_3}{{J_2}^2R_T}sini\left[\left(\frac{3}{2}+2\alpha a+\frac{1}{2}\alpha^2a^2\right)e+\left(-\frac{27}{16}-\frac{5}{2}\alpha a+\frac{1}{8}\alpha^2a^2+\frac{1}{2}\alpha^3a^3+\frac{1}{16}\alpha^4a^4\right)e^3\right]sin\omega\right\}\right\}
\end{aligned}
$$

where

A: drag constant
α: radius vector coefficient in the atmosphere exponential model
μ: Earth´s gravitational constant

5 Non-singular variables

The Eqs. (3) are written such that occur singularity points because of the eccentricity values used for INPE, which uses frozen orbits theory in the CBERS family and in similar satellites (SPOT, Landsat, ERS e IRS). For removing these singularity points, it is necessary to change variables, rewriting Eqs. (3) according to the non-singular variables, ξ and η, what leads eccentricity and argument of perigee to vanish in the explicit form of these equations. The non-singular variables used at INPE CCR can be written as follow

$$\xi = e\cos\omega$$
$$\eta = -e\sin\omega$$

The solution for non-singular variables, according to non-singular theory used at INPE Satellite Tracking and Control Center is

$$
\begin{aligned}
\bar{\xi} &= \xi_0\cos(\omega_1(t-t_0))+(\eta_0+\frac{\xi_2}{\omega_1})sin(\omega_1(t-t_0))+\xi_\Delta(t-t_0)\\
\bar{\eta} &= -\xi_0 sin(\omega_1(t-t_0))+(\eta_0+\frac{\xi_2}{\omega_1})\cos(\omega_1(t-t_0))+\eta_\Delta(t-t_0)-\frac{\xi_2}{\omega_1}
\end{aligned}
\tag{4}
$$

With these informations, Eqs. (3) are rewritten, according to Eqs. (4), and the problem of singularity points vanishes.

6 Method used

Through a program coded in Fortran language and using orbital data of the CBERS-1 satellite, the solution for Eqs. (1) was previously analyzed. The behavior of the solution was compared with the behavior of a known result for other satellite (Cutting et al., 1978). Results have been plotted with MS-Excel graphic editor aid, so that the nature of the frozen orbits could be understood. This feature is extremely important for the users of the images obtained for CCD chamber on board this type of satellite. In fact, the images from different days can be compared for the same latitude being used to preview harvests, fire on forests, to locate underground airports and others utilities.

CBERS-1 has a nominal eccentricity equal to 0.00016. In this paper, we have worked with the frozen orbit that occurs when the argument of perigee is equal to 90º. And we have realized, by graphics, that the orbit starts escaping from its initial path to argument of perigee values far from 90º and has the tendency of standing limited when these values are closer to 90º.

After analyzing the terms which perturbation takes into account J3 terms (already existing), terms of the order of J5 and atmospheric drag were included, in accordance with Eqs. (3). The results were compared with the results for the same equations, but including terms up to J3 only, remembering that all equations were rewritten in terms of non-singular variables (Raimundo, 2004). The results will be shown next.

7 Results and analysis

When we include J5 terms on the perturbations due to the geopotencial, we expect to get greater precision for the frozen elements (argument of perigee and eccentricity). That is, we expect, before anything, a greater prevision capacity of these elements variations, when compared to the variation including only terms up to J3.

When we include perturbations due to the atmospheric drag, we also expect to get greater precision for the frozen elements. That is, we expect, before anything, a greater prevision capacity of these elements variations, when compared to the variation including only terms up to J3 and J5. Adding to that, we expect to verify the atmospheric drag effects on the evolution of the orbital semi-major axis.

Figures (1) and (2) show curves for several initial conditions for the eccentricity and for the argument of perigee. These figures were based on data obtained as the result from Eqs. (2) and (3), both rewritten in non-singular variables. In Fig. (2), geopotential up to J5 terms and atmospheric drag were not included, such terms were included only in the results of Fig. (1). For the atmospheric drag, the solar flux value used was F10.7 of 250. It denotes the maximun solar activity and manifests itself on augmented atmospheric densities and, consequently, on higher drag effects.

Figure (3) shows the secular atmospheric drag effects as a function of time in the semi-major axis. It is noticeable that drag, in the end of the 2.5 long period cycles (300 days), decreases, on a secular way, the semi-major axis around 2 km. It means a reasonable daily rate of decay of 6.64 meters per day, a consistent value because of the high solar activity. Figure (3) still confirms that there isn't long period components affecting the evolution of the semi-major axis.

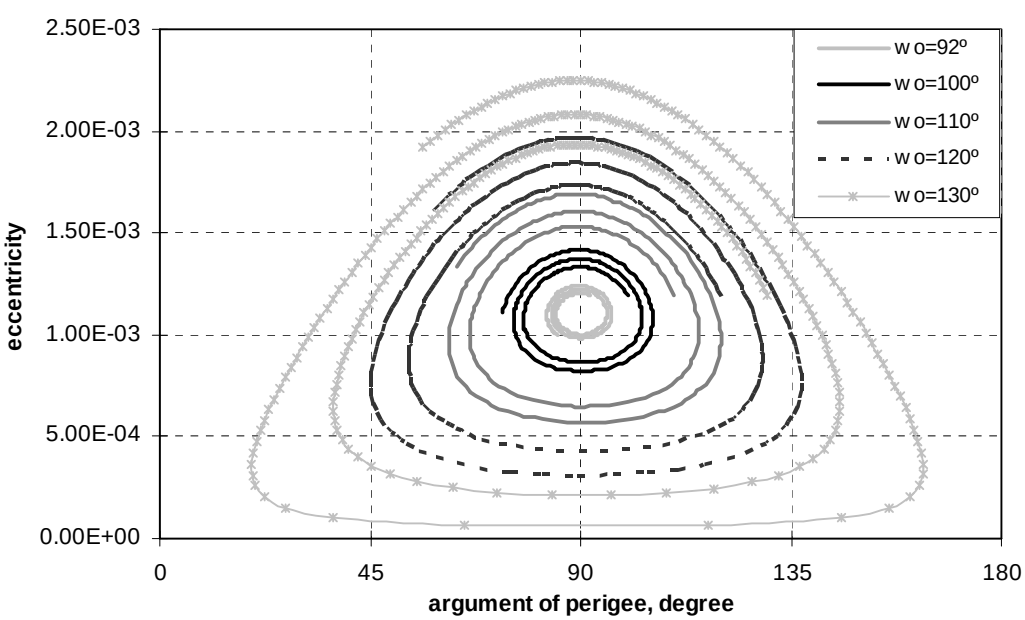

Figure 1. Variation of frozen elements for perturbations due to geopotential up to J5 and atmospheric drag (solar flux = 250) – Non-Singular Theory.

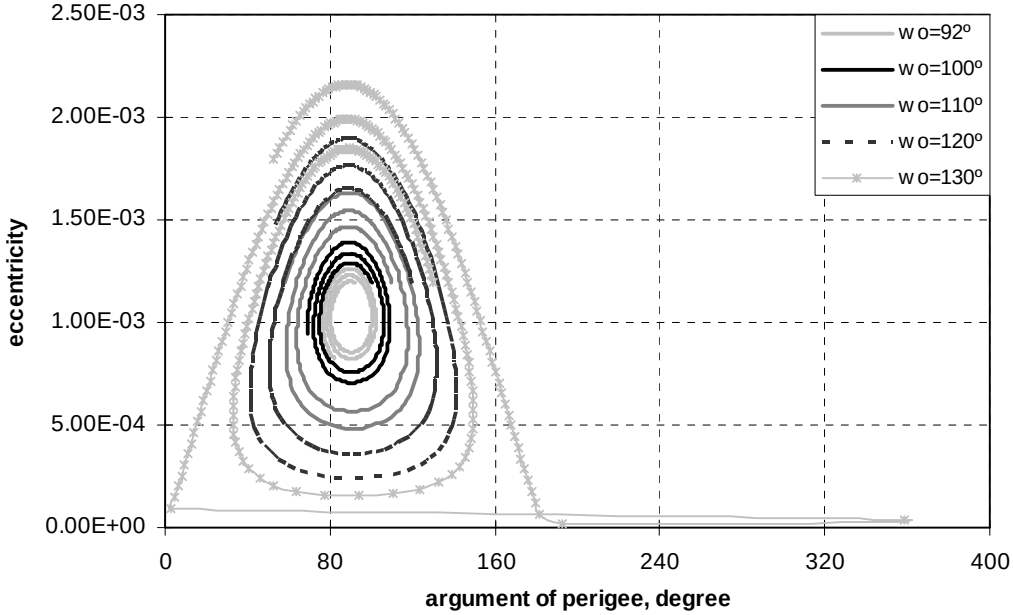

Figure 2. Variation of frozen elements for perturbations due to geopotential up to J3 – Non-Singular Theory.

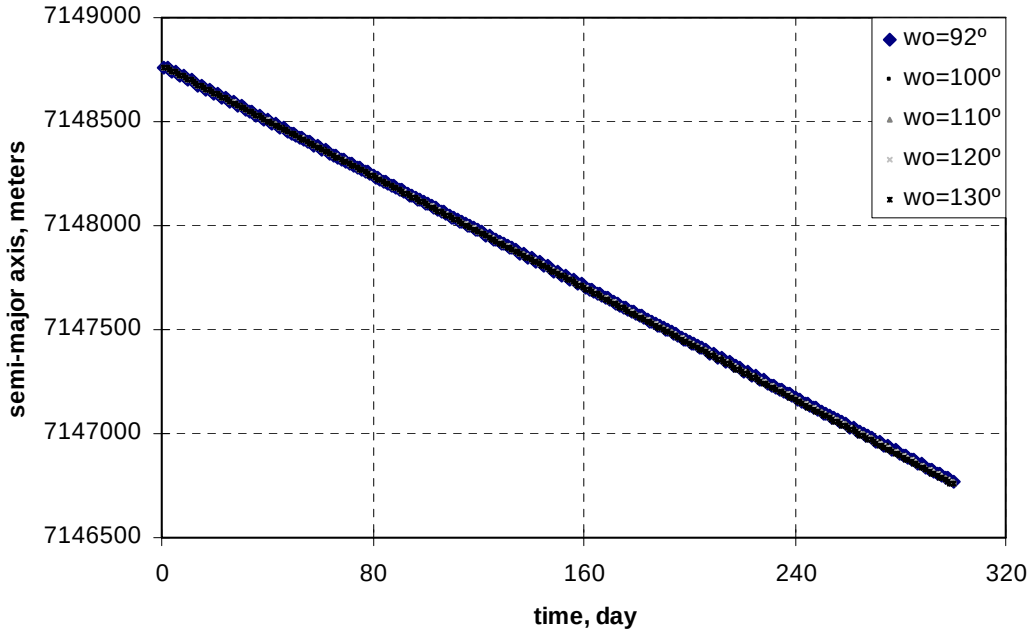

Figure 3. Variation of semi-major axis for perturbations due to atmospheric drag only – Non-Singular Theory.

Figures (1) up to (3) show CBERS-1 evolution, and were obtained for the following values of this satellite orbital elements, to a given date:

- semi-major axis (a) = 7148.763 km
- eccentricity (e) = 0.0011934
- orbital inclination (i) = 98.4896º
- argument of perigee (ω): starting from 90º and variating up to 130º

From the analysis of those figures, it is perceptible that the curves of Fig. (1) have less amplitude of variation for frozen elements, argument of perigee and eccentricity, than the curves of Fig. (2). Just a graphic analysis is not enough to ensure that the inclusion of J5 terms and atmospheric drag effects actually improves the precision. Thus, we construct a table considering several initial conditions for the argument of perigee. This table shows the amplitude of the variations of the argument of perigee and of the eccentricity. From this table, we can observe the decreasing of the amplitudes (in numerical values) when the perturbations due to geopotencial up to J5 are included.

Table 1. Comparative table between the results obtained by J3 and by J3+J5+drag.

Initial Conditions		**Perturbations due to J3**				**Perturbations due to J3+J5+drag**			
e_0	ω_0	Min. Δe	Max. Δe	Max. $\Delta\omega$ (degree)	Max. $\Delta\omega$ (degree)	Min. Δe	Max. Δe	Max. $\Delta\omega$ (degree)	Max. $\Delta\omega$ (degree)
1.193 E-03	90.0º	-2.32E-04	2.10E-04	-12.03	13.58	-1.35E-04	-1.23E-04	-6.57	7.32
1.193 E-03	100.0º	-3.86E-04	2.98E-04	-20.20	20.14	-3.35E-04	2.59E-04	-16.36	15.83
1.193 E-03	110.0º	-6.81E-03	4.71E-04	-31.25	33.50	-6.58E-04	4.64E-04	-28.52	29.73
1.193 E-03	120.0º	-1.02E-03	6.40E-04	-49.50	50.74	-1.01E-03	6.50E-04	-45.92	46.11
1.193 E-03	130.0º	-1.36E-03	7.85E-04	-90.56	265.75	-1.37E-03	8.10E-04	-72.32	71.17

From Table 1 we realized that the amplitude of the variation for the argument of perigee, when geopotential terms of order of J5 and atmospheric drag terms are included, both maximum and minimum amplitudes decrease. This is true for all initial conditions considered. For values of argument of perigee far from the frozen conditions, the values including J5 and drag still complete the cycle, while the cycle with J3 start demeaning (see Fig. (2)). That is, the inclusion of the effects due to J5 and drag improves the precision for the prevision of the argument of perigee. With respect to the eccentricity, the reduction is subtler, but it still occurs.

In practice, the theory using only terms factored up to J3 can persuade to wrong needs of orbital maneuver corrections. If we suppose, for instance, that the mission requires a perigee value between 90º ± 10º, the J3 theory would foresee a corrective maneuver, while the theory including J5 and drag theory exclude the need of a maneuver, as can be seen on the first line of Table (1). So, the conclusion is that it is imperative the inclusion of geopotential terms up to J5 and atmospheric drag terms to improve the precision on planning of maneuvers carry out by INPE Satellite Tracking and Control Center.

8 Conclusions

Brouwer theory using only J3 term can lead to mistaken necessities of orbital correction maneuvers. Assuming that the mission requires an argument of perigee staying around 90° ± 10°, the theory with J3 term foresees one correction maneuver, whilst the theory including J5 term exclude the need of such maneuver. In this manner, by including perturbations due to J5 geopotencial coefficients, we got improvements for precise previsions of frozen elements "ω" and "e". It means a better performance in the orbital operations conducted at the INPE Satellite Tracking and Control Center.

When atmospheric drag is included, there is a higher precision in the frozen elements, in the computation and in the prevision of INPE CRC maneuvers. It was verified that drag introduces a secular component and a long period component with sinusoidal profile and amplitude exponentially crescent. To consider or not atmospheric drag, has matter of considerable impact on long time periods.

On the analysis of drag effects in the semi-major axis, it was found that the influence occurs by decreasing, with a secular component, the magnitude of the semi-major axis. The value of the lessening on a certain interval of time can vary a lot, in accordance with the atmospheric conditions and solar activity considered.

9 Acknowledgements

The authors wish to express their appreciation for the support provided by FAPESP (National Council for Scientific and Technological Development) of Brazil and INPE (Brazilian Institute for Space Research).

10 References

Brouwer, D.: "Solution of the Problem of an Artificial Satellite, Theory without Drag". Astronomical Journal, 64, nº 9, pp. 378-397, 1959.

Brouwer, D. and Hori, G. I.: "Theoretical Evaluation of Atmospheric Drag Effects in the Motion of an Artificial Satellite". The Astronomical Journal, 66, nº 5, pp. 203-205, 212-213, 264-265, 1961.

Cutting, E., Born, G. H. and Frautnick, J. C.: "Orbit Analysis for SEASAT-A". The Journal of Astronautical Sciences, 26, nº 4, pp. 315-342, Oct. – Dec., 1978.

Kovalevsky, J.: "Introduction to Celestial Mechanics". D. Reidel Publishing Company, Netherlands, 1967.

Raimundo, P. C. P.: "Estudos de Elementos Orbitais nas Vizinhanças de uma Órbita Congelada". Final Report of Scientific Iniciation Project. FAPESP, 2004.

Roy, A. E.: "Orbital Motion". Adam Hilger, London, 1988.

Szebehely, V. G. and Mark, H.: "Adventures in Celestial Mechanics". J. Wiley & Sons, New York, 1998.

Von Zeipel, H.: "Recherches sur le Mouvements des Petites Planètes". Arkiv. Mat. Astro. Fysik, 11, 1916.